

**DESIGN WITH CONSTRUCTAL THEORY:
VASCULARIZED AND DISTRIBUTED ENERGY SYSTEMS**

S. Lorente
National Institute of Applied Sciences
Laboratory of Materials and Durability of Constructions
31077 Toulouse, France

A. Bejan
*Author for correspondence
Department of Mechanical Engineering and Materials Science
Duke University
Durham, NC 27708-0300, USA
E-mail: dalford@duke.edu

ABSTRACT

In this paper we use two developments to illustrate our progress in “design with constructal theory” [1]. The first is the development of smart materials with embedded vasculatures that provide multiple functionality: volumetric cooling, self-healing, enhanced apparent (effective) thermal conductivity, and mechanical strength. Vascularization is achieved by using tree-shaped (dendritic) flow architectures. We show that as length scales become smaller, dendritic vascularization provides dramatically superior volumetric bathing than the use of bundles of parallel microchannels. A novel dendritic architecture has trees that alternate with upside down trees. In addition to flow access to the entire volume, trees offer improved robustness in flow operation. The second development is the distributing of energy systems over a given territory. The distribution of heating is used as an example. The architecture emerges from the balancing of the losses concentrated in the production centers and the losses distributed along the conduits that distribute and collect every thing that flows on the landscape. In sum, flow architectures are derived from principle, in accordance with constructal theory, not by mimicking nature.

INTRODUCTION

The current literature reveals a surge of interest in bio-inspired designs of flow architectures that promise superior properties, for example, distributed and high-density heat and mass transfer. Chief among the new architectures that are being proposed are the tree-shaped (dendritic) designs. A significant stimulus for this new direction is the emergence of constructal theory as a means to explain biological and

geophysical design, and as a method for developing new concepts for engineered flow architectures. This growing research activity was reviewed most recently in Refs. [1-3] and is not reviewed again here.

Tree-shaped flow structures have multiple scales that are distributed nonuniformly through the flow space. Tree flows are everywhere in natural flow systems, and their occurrence can be deduced based on a physics principle [the constructal law: “For a finite-size flow system to persist in time (to live) it must evolve in such a way that it provides easier and easier access to the currents that flow through it”]. The constructal law has become an addition to the thermodynamics of nonequilibrium systems: the thermodynamics of flow systems with configuration [4, 5].

“Vascularized” is a good name for the energy systems that the new thermodynamics covers. The tissues of energy flows, like the fabric of society and all the tissues of biology are designed (patterned, purposeful) architectures. The climbing to this high level of performance is the transdisciplinary effort: the balance between seemingly unrelated flows, territories, and disciplines. This balancing act—the optimal distribution of imperfection—generates the very design of the process, power plant, city, geography and economics.

Natural porous flow structures also exhibit multiple scales and nonuniform distribution of length scales through the available space. Can such heterogeneous flow structures be derived from the same principle of maximization of flow access?

In this article we illustrate our recent progress in developing constructal theory and design [1]. In the first example, we show the superior properties of a novel dendritic

flow architecture (Fig. 6) consisting of alternating trees [6]. In the second example we take the multi-scale geometric approach of constructal theory to the global level, and illustrate the emergence of hierarchy in distributed energy systems over the landscape.

NOMENCLATURE

a, b	coefficients, Eqs. (21) and (26)
A, A ₀	areas, m ²
c, d	dimensions, m, Fig. 2
D	diameter, m
f	friction factor
L	length, m
m	mass, kg
\dot{m}	mass flow rate, kg/s
n	number of pairing levels
N	number of parallel channels
N	number of users, Eq. (24)
Po	Poiseuille constant, Eq. (7)
q	heat current, W
R	global flow resistance
Re _D	Reynolds number
S	area, m ²
U	heat transfer coefficient, W/m ² K
U	mean velocity, m/s
V	total flow volume, m ³
x, y	dimensions, m, Fig. 4
Greek letters	
α	angle
ΔP	pressure difference, Pa
ΔT	temperature difference, K
ν	kinematic viscosity, m ² /s
ρ	density, kg/m ³
$\sigma_{1,2}$	sums
Subscripts	
c	critical
i	pairing level
min	minimum
opt	optimum
p	pipe
l	one user

LINE-TO-LINE TREE FLOW

In Fig. 1, each tree connects a point with a straight line. The need to install trees that alternate with upside-down trees comes from the rectangular shape of the line-to-line space.

Consequently, each line is crossed by flows from the many (smallest) canopy channels, which alternate with large streams that flow through the tree trunks. The scales are nonuniformly distributed within each tree, throughout the line-to-line space, along each of the boundaries, i.e. everywhere.

This alternating sequence of point-to-line trees constitutes line-to-line vasculature between the two parallel boundaries of the designed porous body. The fluid flows in the same direction through all the trees, e.g., upward in Fig. 1. This type of vascularization (line-to-line trees) establishes a multiscale “designed porous medium” between the long parallel boundaries of the vascularized body.

The maximization of flow access between the points of one line and the points of a parallel line can be viewed as a sequence of point-to-line flow access maximization problems (Fig. 1). The building block on which Fig. 1 is based was proposed by Lorente et al. [7], where it was constructed by using optimally shaped rectangular areas, as shown in Fig. 2. Because the pressure drop is proportional to the duct length, the rectangular shape d/c was chosen such that the length of the duct PQ that cuts across the fixed area A_0 is minimum. This yielded the shape $d/c = 2$, which led to 90° angles between tributaries, and to collinear ducts on the extremities of the V-shaped tree structure.

The 90° angles deduced in Fig. 2 are an approximation of the best (“equilibrium” [4]) flow structure that could be traced between one point and the many points of a line. To see this, consider the building block sketched in Fig. 3, and abandon the assumption that the stem L_1 and the extreme branch L_2 are collinear. In general, α_1 is not the same as α_2 . The way in which the two branches (or tributaries) cut the upper boundary of the rectangular area S indicates that the Y construct of Fig. 3 is equivalent to a construct that is two-layers thick in Fig. 2.

Assume further that all the tubes are round and with Poiseuille flow, and that they are sufficiently slender so that pressure losses at the junctions can be neglected. In this case, the minimization of the pressure drop across the entire Y-shaped construct (subject to fixed total tube volume) yields the well known Hess-Murray law, according to which the ratio of successive tube diameters is $D_1/D_2 = 2^{1/3}$, regardless of the way in which the tubes are arranged on S .

The optimization of the tube layout is next, and is subjected to holding the area S fixed, while the shape of S may vary. After the optimized D_1/D_2 ratio is substituted into the global pressure drop expression, the global pressure drop is proportional to the geometric flow-resistance group

$$R = L_1 + 2^{1/3} L_2 \quad (1)$$

There are two degrees of freedom in the morphing of Fig. 3, the angles α_1 and α_2 , or one angle and the aspect ratio of S . The

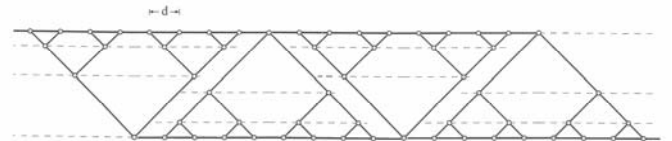


Figure 1 Tree architecture for connecting the points of one line with the points of another line [6].

minimization of R subject to $S = \text{constant}$ is performed numerically, and the results are

$$\alpha_1 = 40.86^\circ \quad \alpha_2 = 53.11^\circ \quad (2)$$

and the minimized global resistance factor (1) is

$$R = 1.3235 S^{1/2} \quad (3)$$

How much better is this bent-Y structure (Fig. 3) relative to the 45° structure of Fig. 2? The answer is readily obtainable from Eq. (1), in which we substitute $L_2 = L_1/2$ and, after some algebra, $L_1 = (2S/3)^{1/2}$:

$$R = (1 + 2^{-2/3}) (2/3)^{1/2} = 1.3309 S^{1/2} \quad (4)$$

Comparing Eq. (4) with Eq. (3) we see that the performance of the simpler (minimum-length) structure of Fig. 2 approaches within 0.5 percent the performance of the more flexible structure optimized in Fig. 3. Such conclusions are reached often in constructal theory: non-equilibrium flow architectures come reasonably close to the equilibrium flow architectures. They come close in terms of performance, even though they may look different.

Because of the comparison made above, in what follows we retain the simpler building blocks sketched in Fig. 2, and with them we explore several ways in which to maximize line-to-line flow access (Fig. 1). Unlike in Fig. 2, we assume a large number of bifurcation levels ($i = 1, 2, \dots, n$), as shown in Fig. 4. Because of symmetry about the bisector of the 2α angle, the tube lengths decrease by a factor of $1/2$, from the largest (L_0), to $L_1 = L_0/2$, $L_2 = L_1/2$, etc. The smallest length scale is the smallest tube length,

$$L_n = 2^{-n} L_0 \quad (5)$$

or the distance between the two ends of two neighboring L_n tubes,

$$d = 2 L_n \sin \alpha \quad (6)$$

In this analysis, we carry α as a parameter, although according to the preceding discussion the value of α should be 45° .

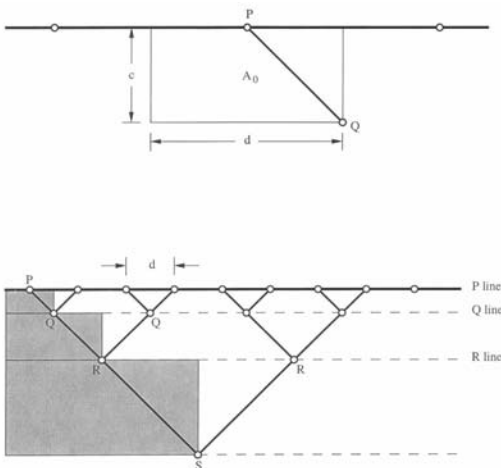


Figure 2 Tree architecture for connecting one point with one line: the length of every duct is minimized [14].

The pressure drop along one tube of length L_i and diameter D_i is

$$\Delta P_i = \dot{m}_i \frac{8}{\pi} \text{Po} \nu \frac{L_i}{D_i^4} \quad (7)$$

where Po is the Poiseuille constant (e.g., $\text{Po} = 16$ for round tubes), which appears in the formula for the friction factor,

$$f_i = \frac{\text{Po}}{\text{Re}_{D_i}} \quad (8)$$

and $\text{Re}_{D_i} = U_i D_i / \nu$ with $U_i = \dot{m}_i / (\rho \pi D_i^2 / 4)$. Mass conservation at every junction requires that $\dot{m}_i = 2\dot{m}_{i+1}$, where it is again assumed that the tubes are sufficiently slender so that the asymmetry of the Y junction does not affect the splitting of \dot{m}_i into two equal streams \dot{m}_{i+1} . After using the ratios for diameters, lengths and mass flow rates indicated above, the total pressure drop from the open end of the L_0 tube to the open ends of the L_n tubes, becomes

$$\Delta P = \sum_{i=1}^n \Delta P_i = \dot{m}_0 \frac{8}{\pi} \nu \text{Po} \frac{L_0}{D_0^4} \sigma_1 \quad (9)$$

where $\sigma_1 = 1 + 2^{-2/3} + \dots + 2^{-2n/3} = [1 - (2^{-2/3})^{n+1}] / (1 - 2^{-2/3})$.

The total tube volume occupied by the tree flow is

$$V = \frac{\pi}{4} (D_0^2 L_0 + 2D_1^2 L_1 + \dots + 2^n D_n^2 L_n) = \frac{\pi}{4} D_0^2 L_0 \sigma_1 \quad (10)$$

The largest length scale (L_0) is related to the vertical dimension of the tree (y) by

$$y = (L_0 + L_1 + \dots + L_n) \cos \alpha = L_0 \sigma_2 \cos \alpha \quad (11)$$

where $\sigma_2 = 2 [1 - 2^{-(n+1)}]$. The horizontal dimension (x) of the area occupied by the tree projection is

$$x = 2^n d = 2 L_0 \sin \alpha = \frac{2}{S_2} y \tan \alpha \quad (12)$$

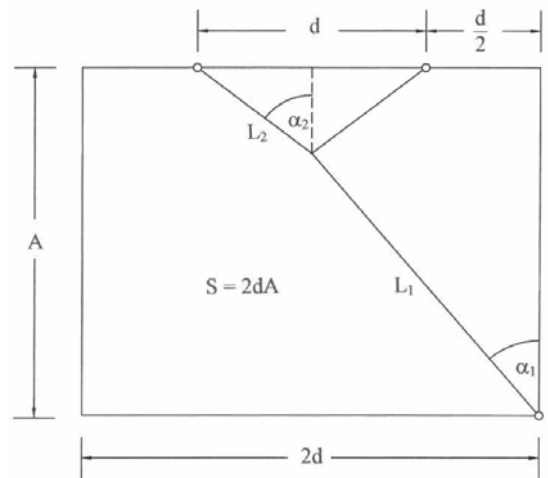


Figure 3 Y-shaped construct in which, in general, α_1 is not the same as α_2 [6].

where 2^n is the number of L_n tubes that reach the upper end of the construct. Eliminating L_0 and D_0 between Eqs. (9) – (11) we obtain

$$\Delta P = \dot{m}_0 \frac{\pi}{2} P_0 \frac{v}{V^2} \left(\frac{\sigma_1 y}{\sigma_2 \cos \alpha} \right)^3 \quad (13)$$

We question how effective the tree structure of Fig. 4 is relative to a well-known reference architecture: an array of N equidistant parallel tubes, each of length y and diameter D . This classical structure carries the same total flow rate \dot{m}_0 in the same total tube volume ($V = N \frac{\pi}{4} D^2 y$) and over the same area $xy/2$. The structure has one degree of freedom, the tube diameter D , or the number of parallel tubes,

$$N = \frac{4V}{\pi D^2 y} \quad (14)$$

The pressure drop along this structure (ΔP_{ref}) is the same as the pressure drop along a single tube, cf. Eq. (7), through which the flow rate now is \dot{m}_0/N ,

$$\Delta P_{\text{ref}} = \frac{\dot{m}_0}{N} \frac{8}{\pi} P_0 v \frac{y}{D^4} \quad (15)$$

Eliminating D by using Eq. (14) we obtain

$$\Delta P_{\text{ref}} = \dot{m}_0 \frac{\pi}{2} P_0 \frac{v}{V^2} N y^3 \quad (16)$$

The tree-shaped structure of Fig. 4 has a smaller flow resistance than the parallel channels when $\Delta P < \Delta P_{\text{ref}}$, or, using Eqs. (13) and (16), when

$$N > \left(\frac{\sigma_1}{\sigma_2 \cos \alpha} \right)^3 \quad (17)$$

The right side of this inequality is a number on the order of 1.

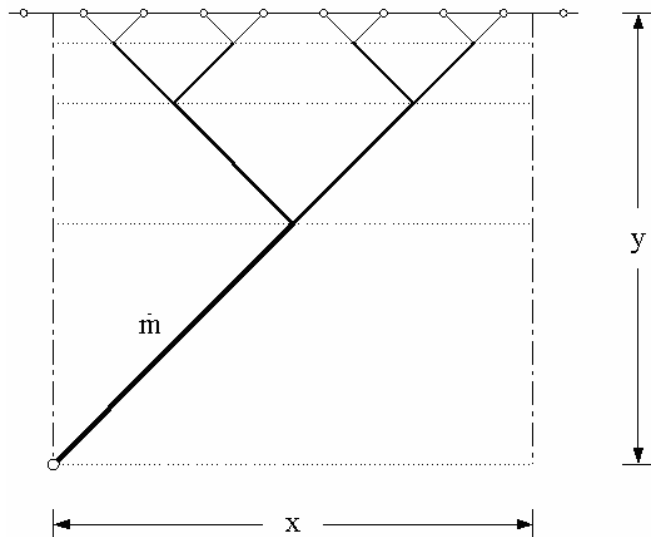


Figure 4 One of the point-to-line trees of Fig. 1 [6].

In conclusion, as the reference structure becomes finer (i.e., as N increases), the tree-shaped design of Fig. 4 becomes more attractive.

This conclusion can be read as a statement of how fine the tree structure must be such that it is preferable to the reference design. For a more practical comparison, assume that the smallest dimension that can be manufactured (d) is the same in both architectures, i.e. the d spacing of Fig. 4 is the same as the spacing between parallel tubes. This means that the number of parallel channels that occupy the area $y \times (x/2)$ is $N = 2^n/2$, and when $\alpha = 45^\circ$ the inequality (17) becomes approximately

$$\frac{\Delta P}{\Delta P_{\text{ref}}} \cong \frac{14}{2^n} < 1 \quad (18)$$

We conclude that when the number of branching levels is 4 or larger, the tree-shaped architecture offers greater access to the flow that permeates through the porous structure of thickness y . The superiority of the tree design increases fast as n increases: when $n = 7$, the ratio $\Delta P/\Delta P_{\text{ref}}$ is as low as $1/10$.

Tree-shaped flows occur everywhere, not only for fluid flow access but also for energy, goods, people, etc. [8]. In Ref. [9] we explored the use of line-to-line trees for configuring counterflow heat exchangers with greater volumetric density of heat transfer [9].

DISTRIBUTED ENERGY SYSTEMS

One lesson that nature teaches us is that in highly complex systems the generation and use of motive power is *distributed* throughout the body. It is not centered in a single spot, nodule or organ. The animal muscle is a “tapestry” of patches served by two kinds of flow systems: (i) tissues that generate movement (contraction), and (ii) vascularization that feeds, cleanses and endows the tissue with the ability to sense and act.

So perfect is the allocation of power generation to the networks for supply and distribution that the untrained eye sees the tissue as one, or, at the most, as a complicated (multiscale) porous flow structure. The “allocating” of one flow system to the other flow system, in the same confined space, is the secret of the design. How are such designs made? How do they function?

These questions are interesting and highly promising when placed in the context of a sustainable energy future for our planet. The inhabited surface of the earth is covered by the same two classes of flow systems: (i) nodules, large channels of power generation, embedded in (ii) networks of supply and distribution. Systems (i) and (ii) are allocated to elemental areas forming a patchwork that covers countries and continents. For example, the air mass-transit map has history and memory. In time, new channels appear and old ones become thicker.

Like the animal muscle, the patchwork of power generation, distribution and use happened *naturally*. Unlike the animal muscle, which has spent millions of years in the factory of evolution, our energy systems evolve in front of our eyes. They morph while they grow. They produce more power, and they produce the power more efficiently. Why do humans need power? For the same reason that animals need muscle power: to move mass on the earth’s surface. Recent theoretical work

on the origins of animal locomotion [10, 11] has shown that for all types of locomotion (running, flying, swimming), animal force is roughly equal to the body weight, and the minimum work that the body performs is proportional to the body weight times the distance traveled. The consumed food or fuel is “converted” into mass moved. Our cars, construction sites and everything else we do (our legacy) are the product of this. All the animals and all of us consume food and fuel, and the result is the shaping and reshaping (the mixing) of the earth’s surface.

The widespread occurrence of *distributed* energy systems in nature is a very loud hint that the future of human energy design belongs to distributed systems. *The future belongs to the vascularized.* In nature, distributed energy systems occur not only in animal design but also in inanimate flow systems such as river basins. Each sloped channel in a river basin is an optimal combination of (i) motive power (the slope, i.e., the driving gravitational potential), (ii) distribution, use, dissipation (friction along the channel), and the allocation of (i) and (ii) to the elemental territory bathed by the channel. The time arrow of evolution in natural flow systems points toward distributed energy systems.

Here we show how to uncover the most fundamental principles of distributed energy systems—what makes them more efficient, more resilient and more adaptable than other architectures. We search for the principles that govern the generation of patterns, clusters of energy systems, centralization vs. decentralization, and transitions (in time) from one configuration to another. We start from the simplest setting for pursuing the above questions, and look toward more complex, more realistic and more interdisciplinary manifestations of the *phenomenon* of distributed energy design.

Consider the design of energy systems for heating. Humanity needs heating all over the globe, and for this reason the burning of fuel occurs all over the globe. Key is the observation that all the generated heat (the used and the unused) is eventually discharged into the environment. The challenge is to channel most of this heat through our homes and enterprises before discharging it into the environment. The challenge is to place humans and enterprises in the right places on the landscape, as optimally positioned interceptors. When this tapestry of interceptors of heat is designed from principle, two major objectives are achieved simultaneously:

- The heating needs of humanity are met by burning minimum fuel, and
- The total heating dumped into the environment is the smallest that it can be.

To illustrate the approach, assume that our heating needs are served by streams of hot water of temperature $T_\infty + \Delta T$, where T_∞ is the environment temperature, and ΔT is specified. These streams are heated in imperfect installations that burn fuel, heat water, and leak a portion of the heat of combustion to the environment.

The hot water is used by individuals and their enterprises at discrete sites (Fig. 5a-c). Assume that all the sites are identical in size and need. Size is indicated by the length scale of one site, d , which is fixed. Need is indicated by the hot water mass m_1 used per unit time at one site. The following scale analysis refers to hot water generation and use on a per unit time basis.

According to the rules of scale analysis, factors of order 1 are neglected, and the results are correct and accurate within a factor of order 1.

Consider two designs for distributing water heating and use. First, every user produces its hot water on site in a heater-tank installation. An individual water heating tank is modeled as a sphere of diameter D_1 . This tank is filled with hot water (mass m_1), and leaks heat to the ambient in proportion to the tank surface,

$$q_1 \sim U D_1^2 \Delta T \quad (19)$$

where U is the overall heat transfer coefficient (between water mass and ambient) multiplied by the time unit. In view of the tank size, $m_1 \sim \rho D_1^3$, where ρ is the water density, the heat loss from the water tank is

$$q_1 \sim U \left(\frac{m_1}{\rho} \right)^{2/3} \Delta T \quad (20)$$

There are N user sites on the territory of size A . The total heat loss from the N sites is

$$q = N q_1 \sim a N m_1^{2/3} \quad (21)$$

where $a = U \rho^{-2/3} \Delta T$. We see that the loss of fuel burned (q) is proportional to the size of the population (N) and the individual water consumption raised to the power $2/3$. Can this penalty be made smaller? The answer is yes, and the solution consists of *organizing* the users on the landscape. One design with organization is where N users are arranged around a single water-heating site. The central tank has the size

$$m_c = N m_1 \quad (22)$$

and the heat loss, cf. Eq. (21),

$$q_c \sim a m_c^{2/3} \quad (23)$$

The N users are positioned on a circle of radius L , therefore

$$L \sim N d \quad (24)$$

Each user receives its hot water allocation (m_1) through an L -long radial pipe of standard diameter D_p . Each pipe loses heat in amount

$$q_{lp} \sim U_p D_p L \Delta T \quad (25)$$

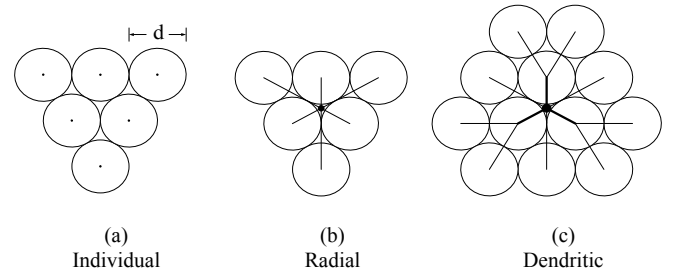


Figure 5 Distributed energy systems for heating: (a) Individual heaters; (b) Central heater and radial distribution lines; (c) Central heater and dendritic distribution network.

where U_p is the pipe-ambient heat transfer coefficient multiplied by the time unit. The loss from the N radial pipes is

$$q_p = Nq_{1p} \sim bLN \quad (26)$$

where $b = U_p D_p \Delta T$. The global loss from the entire construct (central heater + radial pipes) is

$$q \sim q_c + q_p \quad (27)$$

The global loss per user is

$$\frac{q}{N} \sim \frac{am_1^{2/3}}{N^{1/3}} + bNd \quad (28)$$

This expression shows that the density of heat loss is minimum when the number of users grouped around a single central heater is

$$N_{\text{opt}} \sim \left(\frac{a}{bd}\right)^{3/4} m_1^{1/2} \quad (29)$$

The minimum heat loss density is

$$\left(\frac{q}{N}\right)_{\text{min}} \sim a^{3/4}(bd)^{1/4} m_1^{1/2} \quad (30)$$

The significance of this result becomes evident when we compare it with Eq. (21), where $q/N \sim am_1^{2/3}$. In both designs, q/N increases with the individual water use, but the rate of increase depends on m_1 . This is shown in Fig. 6, where the abscissa can be interpreted as the direction of time, or the direction of increase in living standard (namely, amount of hot water use per unit time). When m_1 is small, preferable is the decentralized design: one heater on every site. When m_1 is sufficiently large, preferable is the centralized water heating and site. When m_1 is sufficiently large, preferable is the centralized water heating and distribution design. The *transition* between the two designs occurs when m_1 reaches the

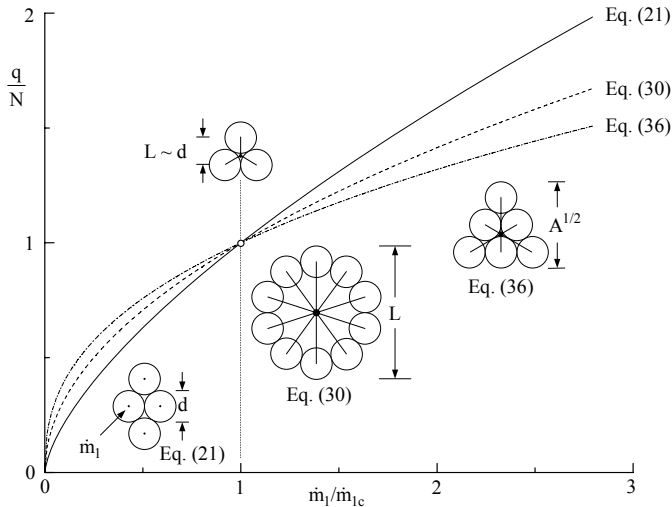


Figure 6 The fuel burned per user in three configurations: individual heaters, central heater with radial lines to users on a circle, and central heater with radial lines to users clustered near the heater.

critical size

$$m_{1c} \sim \left(\frac{bd}{a}\right)^{3/2} \sim \rho \left(\frac{U_p D_p d}{U}\right)^{3/2} \quad (31)$$

for which the critical number of organized sites is:

$$N_c \sim 1 \quad (32)$$

The geometric meaning of $N_c \sim 1$ is derived from Eq. (24), which now reads

$$L_c \sim d \quad (33)$$

In conclusion, at transition the users should cluster tightly at a distance of order d around a central source. Arrangements of this type are triangular ($N = 3$), square ($N = 4$), hexagonal ($N = 6$), e.g., Fig. 5b. Larger clusters ($N > N_c$) are more attractive when m_1 becomes greater than m_{1c} .

When the m_1 sites are tightly packed, the minimization of q/N is synonymous with the minimization of the loss per unit territory, q/A . When $m_1 > m_{1c}$, the radial scale L exceeds d , and the area (of order L^2) is covered only partially by user sites (area of order Ld).

If land is at such a premium that it is covered continuously by users, then Eqs. (22) - (33) can be repeated for an area A covered completely by N sites of size d , namely $A \sim Nd^2$. The length scale of area A is then $L \sim A^{1/2} \sim N^{1/2}d$. This is the length scale of any of the pipes connecting one user to the single hot-water generation center located on A . Substituting $N^{1/2}d$ in place of L in Eq. (26) we obtain $q_p \sim bN^{3/2}d$. In place of Eq. (28) we write

$$\frac{q}{A} \sim \frac{am_1^{2/3}}{d^2 N^{1/3}} + \frac{b}{d} N^{1/2} \quad (34)$$

The optimal number N for minimum q/A is

$$N_{\text{opt}} \sim \left(\frac{a}{bd}\right)^{6/5} m_1^{4/5} \quad (35)$$

for which Eq. (34) yields

$$\left(\frac{q}{A}\right)_{\text{min}} \sim b^{2/5} a^{3/5} d^{-8/5} m_1^{2/5} \quad (36)$$

Written in terms of q/A , Eq. (21) becomes

$$\frac{q}{A} \sim \frac{a}{d^2} m_1^{2/3} \quad (37)$$

The transition between the disorganized design (37) and the organized design (36) occurs at the intersection of the two, which is the same as in Eq. (31). This is to be expected, because when $m_1 \leq m_{1c}$ the area A is proportional to N .

The next question is what should happen when m_1 exceeds m_{1c} . In this domain, we compare Eq. (36) with Eq. (30) on a q/N basis. The two equations become

$$\frac{q_{30}}{N} \sim bd \tilde{m}_1^{1/2} \quad (38)$$

$$\frac{q_{36}}{N} \sim bd \tilde{m}_1^{2/5} \quad (39)$$

where, in view of Eq. (31), $\tilde{m}_1 = m_1 / m_{1c}$. When $\tilde{m}_1 > 1$, the heat loss minimized in Eq. (36) is smaller than in the design of Eq. (30). This is indicated by the curve drawn for Eq. (36) in Fig. 6.

The chief message of this very simple example is that the emergence of configuration in time can be derived from principle. The drawings and their times of emergence can be *predicted*. Organization is good, provided that the level of advancement (m_1) calls for it. For example, Fig. 6 indicates that when the individual need (m_1) is less than m_{1c} the better configuration is the individual pattern (Fig. 5a). When m_1 increases above the critical level, the preferred pattern is radial and tightly packed (Fig. 5b).

The constructal literature [1] suggests that farther in time (i.e., to the right in Fig. 6) we will discover even better configurations, such as the dendritic design sketched in Fig. 5c. This is the direction of the constructal paradigm: thinking ahead (in time), and searching *without bias* for the best organization that benefits every member of the organization.

The illustration of the generation of distributed-energy configuration can be thought of as a tradeoff between losses concentrated in the nodes of production and losses spread along the lines of the distribution network. When these two kinds of losses are balanced (i.e., summed up and minimized on the available territory), and when the flow paths are free to morph, the configuration takes shape.

This trade-off generates other important designs. The generation of electricity in power plants is an important application of this approach. Economies of scale are well established in power generation. Larger stationary power plants are more efficient than miniature power plants. The attractiveness of a large power plant makes the clustering of more and more users attractive. At the same time, the territory served by the power plant increases, and so does the length scale of the power distribution lines. The losses due to distributing the power grow as the power plant grows. There is a tradeoff between the savings associated with using a central (efficient) power plant and the losses of a dissipative distribution network. This tradeoff establishes the length scale of the pattern in which power plants must be allocated to users, and how each such cluster must be allocated to its area on the landscape. This is the conceptual route to discovering the architecture of the distributed power system.

SCALING UP

The work line traced in the section on Distributed Energy Systems is a promising direction to solving the toughest of all problems in engineering design: scaling, i.e., how to use the results from a desk-size model in order to predict the behavior and performance of “the same” system but at much larger scales. The difficulty stems from the nature of all flow systems: the larger is not “the same” as the laboratory model. The larger is not a magnified replica of the model.

What happens during the magnification exercise is suggested by the abscissa of Fig. 6. The configuration *changes*,

because the flow system must be the best that it can be *at any size*. One cannot predict the performance of a large-use heating system ($m_1 > m_{1c}$, Fig. 6) by extrapolating from the tested performance of a small-use system ($m_1 < m_{1c}$).

The only way to crack the scaling nut is to have a firm grip on the hammer of principles, i.e., to know how the system configuration changes as its size increases. Once we know the drawing, large or small, we can analyze (or test) the flow system and describe its performance with confidence. This means that if we know that Fig. 5c will be the configuration at large scales, then we must test in the laboratory a miniature of Fig. 5c, not of Fig. 5a. This knowledge is a powerful new tool, and a very timely one for placing the subject of “design” on a scientific basis.

CONCLUSIONS

In this paper we illustrated our progress in using constructal theory for the design of novel flow architectures for energy systems. Two classes were used as examples, vascularized smart composites with line-to-line flow and distributed energy systems. In both, the recommended architecture emerged as a balance between two or more loss mechanisms. In vascular systems, the balance is between the flow resistances distributed over many small channels and few large channels. In distributed systems, the balance is between losses that occur in nodes (points of flow concentration), and losses that are distributed along the lines that connect the nodes.

In sum, this new work provides additional lessons regarding the general applicability of the constructal law and its design principle of “optimal distribution of imperfection”. The latest progress in this domain is detailed in Refs. [1-3, 12].

Acknowledgement. This research was supported by the Air Force Office of Scientific Research based on a MURI grant for the development of “Micro-vascular Autonomic Composites” (University of Illinois at Urbana Champaign, Duke University, and University of California, Los Angeles), and based on a grant for “Constructal Technology for Thermal Management of Aircraft”. We thank Dr. David Moorhouse (Air Force Research Laboratory) for the advice and guidance that he gives us in this research direction.

REFERENCES

- [1] A. Bejan and S. Lorente, *Design with Constructal Theory*, Wiley, Hoboken, 2008.
- [2] A. Bejan and S. Lorente, Constructal theory of generation of configuration in nature and engineering, *J. Appl. Phys.*, Vol. 100, 2006, 041301.
- [3] A. Bejan, *Advanced Engineering Thermodynamics*, 3rd ed., Wiley, Hoboken, 2006, ch. 13.
- [4] A. Bejan and S. Lorente, “The Constructal Law and the Thermodynamics of Flow Systems with Configuration”, *International Journal of Heat Mass Transfer*, Vol. 47, 2004, pp. 3203-3214.
- [5] A. Bejan and S. Lorente, *La loi constructale*. L’Harmattan, Paris, 2005.

- [6] S. Lorente and A. Bejan, Heterogeneous porous media as multiscale structures for maximum flow access, *Journal of Applied Physics*, Vol. 100, 2006, 114909.
- [7] S. Lorente, W. Wechsato and A. Bejan, Tree-shaped flow structures designed by minimizing path lengths, *Int. J. Heat Mass Transfer*, Vol. 45, 2002, pp. 3299-3312.
- [8] A. Bejan and G. W. Merks, eds., *Constructal Theory of Social Dynamics*, Springer, New York, 2007.
- [9] H. Zhang, S. Lorente and A. Bejan, Vascularization with trees that alternate with upside-down trees, *J. Appl. Phys.*, Vol. 101, 2007, 094904.
- [10] A. Bejan and J. H. Marden, Unifying constructal theory for scale effects in running, swimming and flying, *J. Exp. Biol.*, Vol. 209, 2006, pp. 238-248.
- [11] A. Bejan and J. H. Marden, Constructing animal locomotion from new thermodynamics theory, *American Scientist*, July-August, 2006, pp. 343-349.
- [12] www.constructal.org